Angewandte
International Edition Chemie

Chalcogen Bonding

DOI: 10.1002/anie.201405901

The Dominant Role of Chalcogen Bonding in the Crystal Packing of 2D/3D Aromatics**

Jindřich Fanfrlík, Adam Přáda, Zdeňka Padělková, Adam Pecina, Jan Macháček, Martin Lepšík, Josef Holub, Aleš Růžička, Drahomír Hnyk,* and Pavel Hobza**

Abstract: *The chalcogen bond is a nonclassical σ-hole-based noncovalent interaction with emerging applications in medicinal chemistry and material science. It is found in organic compounds, including 2D aromatics, but has so far never been observed in 3D aromatic inorganic boron hydrides. Thiaboranes, harboring a sulfur heteroatom in the icosahedral cage, are candidates for the formation of chalcogen bonds. The phenyl-substituted thiaborane, synthesized and crystalized in this study, forms sulfur⋯π type chalcogen bonds. Quantum chemical analysis revealed that these interactions are considerably stronger than both in their organic counterparts and in the known halogen bond. The reason is the existence of a highly positive σ-hole on the positively charged sulfur atom. This discovery expands the possibilities of applying substituted boron clusters in crystal engineering and drug design.*

The chalcogen bond is a novel type of noncovalent interaction between a chalcogen atom and an electron (e^-) donor.[1–4] It belongs to the family of σ-hole bonding, where the halogen bond (X-bond) is by far the most known. Since chalcogen atoms are electronegative elements, they are usually negatively charged in organic compounds. The chalcogen bond, that is, the bond between a (mostly) negatively charged chalcogen atom and a negatively charged e^- donor, is thus as counterintuitive as the X-bond. Because of the unequal occupation of the valence orbitals at the chalcogen (halogen), the electrostatic potential (ESP) around the chalcogen atom is strongly anisotropic. Therefore, besides the expected negative areas, there are also areas of positive ESP, called σ-holes.[5]

Although the chalcogen bond is not so well researched compared to the X-bond, it plays an important role in crystal engineering and in interactions of drugs or biological molecules.[2,3,6–10] It is important for the biological activity of several organic molecules.[8] An analysis of the Protein Data Bank suggests that the S⋯O interactions influence protein structures.[3,6]

A σ-hole is characterized by its magnitude ($V_{s,max}$) and size.[11] $V_{s,max}$ is defined as the value of the most positive ESP of an e^- density surface and the size as the spatial extent of the positive region. $V_{s,max}$ and the size increases on going from Cl to I or from S to Te. The chemical environment also plays a role. $V_{s,max}$ can be increased by e^--withdrawing groups in the vicinity of the X or chalcogen atom.[4,11,12] As also noticed, the higher the $V_{s,max}$ value is, the stronger is the X-bond. A modulation of the X-bond in protein–inhibitor complexes was used to reduce the IC_{50} values accordingly.[13,14]

Reference interaction energies (ΔE) for the X-bond are obtained using the highly accurate CCSD(T) calculations. Hartree–Fock (HF) and density funtional theory (DFT) usually give too low ΔE values.[12] Their use should thus be verified by the CCSD(T) calculations.

Inherently e^--deficient polyhedral boron clusters (boranes) exhibit an astonishing variety of stable structures. Numerous applications include radioactive waste extraction, nanotechnology and medicinal chemistry.[15–17] The properties which make boranes such suitable entities include their hydrophobicity, shape, 3D aromaticity, stability and ability to form dihydrogen bonds.[18,19] An important class of boranes comprises *closo*-$B_nH_n^{2-}$ (known for $n = 5$–12) dianions. The

---

[*] Dr. J. Fanfrlík,[+] A. Pecina, Dr. M. Lepšík, Prof. P. Hobza
Gilead Sciences Research Center and
Institute of Organic Chemistry and Biochemistry
Academy of Sciences of the Czech Republic, v.v.i.
Flemingovo nám. 2, 16610 Prague 6 (Czech Republic)
E-mail: hobza@uochb.cas.cz

Prof. P. Hobza
Regional Center of Advanced Technologies and Materials
Department of Physical Chemistry, Palacký University
77146 Olomouc (Czech Republic)

A. Přáda,[+] Dr. J. Macháček, Dr. J. Holub, Dr. D. Hnyk
Institute of Inorganic Chemistry
Academy of Sciences of the Czech Republic, v.v.i.
25068 Řež u Prahy (Czech Republic)
E-mail: hnyk@iic.cas.cz

Dr. Z. Padělková,[+] Prof. A. Růžička
University of Pardubice
Studentská 573, 53210 Pardubice (Czech Republic)
E-mail: ales.ruzicka@upce.cz

[+] These authors contributed equally to this work.

[**] This work was supported by research projects RVO 61388963 awarded by the Academy of Sciences of the Czech Republic. We acknowledge the financial support of the Czech Science Foundation (J.F., A.P., M.L., P.H.: grant number P208/12/G016; D.H.: grant number P208/10/2269). We also thank the Gilead Sciences and IOCB Research Centre for financial support. This work was also supported by the Operational Program Research and Development for Innovations—European Science Fund (grant number CZ.1.05/2.1.00/03.0058). This work was supported by the IT4Innovations Centre of Excellence project (CZ.1.05/1.1.00/02.0070), funded by the European Regional Development Fund and the national budget of the Czech Republic via the Research and Development for Innovations Operational Programme, as well as Czech Ministry of Education, Youth and Sports via the project Large Research, Development and Innovations Infrastructures (LM2011033).

Supporting information for this article is available on the WWW under http://dx.doi.org/10.1002/anie.201405901.

BH^{2-} vertices can be formally replaced by isoelectronic CH^{-} or S units and can thus form carboranes or neutral thiaboranes, respectively. Apart from the parent thiaborane, *closo*-1-SB$_{11}$H$_{11}$, its 12-Cl- and 12-I-variants (**Cl-SB$_{11}$** and **I-SB$_{11}$**, respectively) were previously prepared in our laboratories.[20] This prompted us to prepare the thiaborane with an antipodal phenyl *exo*-substitution, 12-Ph-*closo*-1-SB$_{11}$H$_{10}$ (**Ph-SB$_{11}$**), in which 2D and 3D aromatics are connected (see the Supporting Information). These substituted compounds enabled us to analyze the ability of thiaboranes to form chalcogen bonds.

Conceivably, the charge distribution of thiaboranes differs significantly from that of sulfur-containing organic compounds. The comparison of calculated ESPs and dipole moments is shown in Figure 1.

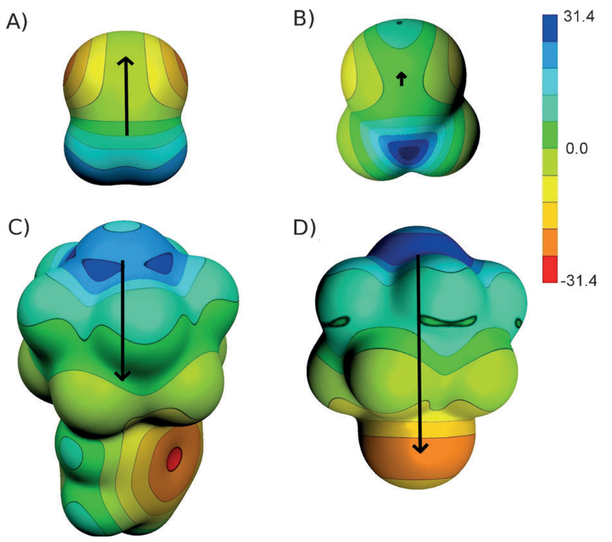

Figure 1. Electrostatic potentials (ESPs) on 0.001 a.u. and dipole moments (arrows) computed at the HF/cc-pVDZ level. The molecular surfaces of A) H$_2$C=S, B) F$_2$C=S, C) **Ph-SB$_{11}$** and D) **Cl-SB$_{11}$**. ESP in kcal mol^{-1}.

The S atom in H$_2$C=S and F$_2$C=S is divalent and negatively charged (Table 1). The evidence of the σ-hole is clearly visible in Figure 1 and Table 1, which show less negative and positive σ-holes in H$_2$C=S and F$_2$C=S, respectively. The key role in this respect is played by two e^{-}-withdrawing F atoms here. The most positive regions are localized at the top of the S atom. In contrast, the S atom in thiaboranes is bound to five B atoms and is thus positively charged (Table 1). Nevertheless, the ESP of **Ph-SB$_{11}$** clearly shows the existence of a less positive top of the S atom and of five highly positive σ-holes on its sides (Figure 1 C). The $V_{s,max}$ is even higher here than in the majority of halogenated compounds. The $V_{s,max}$ of **Ph-SB$_{11}$** is comparable to the $V_{s,max}$ of Br-benzene with several e^{-}-withdrawing groups.[11,12] In **Cl-SB$_{11}$**, the σ-holes are even bigger and joined into a more positive belt, which ranges from 120° to 150° from the B12-S axis. It shows that the properties of σ-holes can be tuned by introducing e^{-}-withdrawing groups on the 3D aromatic cage. Similar tuning of σ-hole properties on the 2D aromatic are well known for X-bonds. These findings have important consequences—the resulting chalcogen bond should be strong and bent, unlike the linear X-bonds. A detailed computational study on σ-hole bonding of heteroboranes is under preparation.

Table 1: The magnitude of σ-holes ($V_{s,max}$), Mulliken partial atomic charges on the S atom (q_s), and dipole moment (μ) in kcal mol^{-1}, e^{-}, and *D*, respectively.

Compound	$V_{\sigma,max}$	q_s	μ
H$_2$C=S	−3.1	−0.12	2.12
F$_2$C=S	12.6	−0.11	0.31
Ph-SB$_{11}$	26.7	0.13	3.29
Cl-SB$_{11}$	30.7	0.13	5.31[a]

[a] The experimental μ of **Cl-SB$_{11}$** is 5.49 D.[20]

The **Ph-SB$_{11}$** compound was synthesized and crystallized (see the Supporting Information). The crystal structure (Figure 2 A) showed several interaction motifs (Figure 2 D) which were investigated using advanced methods of quantum chemistry (QM) and compared with crystal structures of **Cl-SB$_{11}$** and **I-SB$_{11}$** (Figure 2).[20]

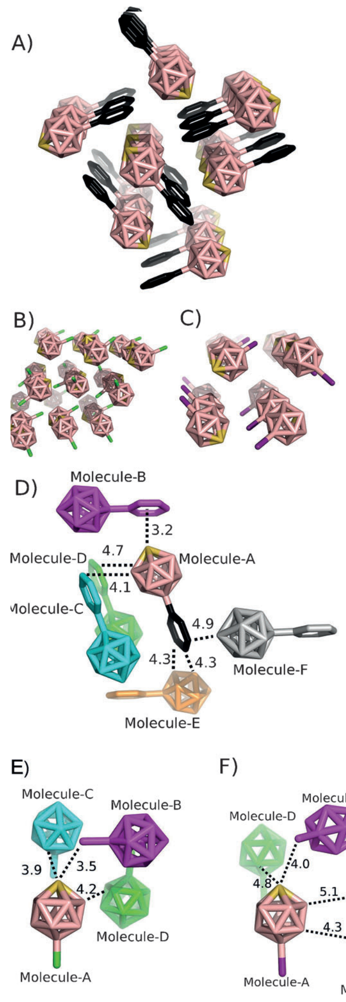

Figure 2. The crystal structures (A, B, C) and the most stable interactions (D, E, F) in the crystals of **Ph-SB$_{11}$** (A, D), **Cl-SB$_{11}$** (B, E), and **I-SB$_{11}$** (C, F). A, B, C and the central molecules in D, E, F colored by element (pink: B, yellow: S, black: C, green: Cl, magenta: I). H atoms omitted for clarity.

Table 2: The interaction energies (ΔE) and their decomposition into the electrostatic (E_1^{pol}), exchange-repulsion (E_1^{exch}), dispersion (E^{disp}), and induction (E_1^{ind}) terms; all in kcal mol^{-1}.

Motif	DFT-D3/CCSD(T)	DFT-SAPT				
	ΔE	E_1^{pol}	E_1^{exch}	E^{disp}	$E^{\text{ind[a]}}$	ΔE
		Ph-SB$_{11}$				
A-B	−8.2/−8.6	−5.8	10.8	−12.0	−2.0	−8.8
A-C	−7.4/−7.3	−2.8	9.4	−14.8	−0.8	−9.1
A-D	−5.5/−5.4	−2.4	7.5	−11.2	−0.5	−6.6
A-E	−2.6	−0.7	2.2	−4.3	−0.2	−3.0
A-F	−2.0	−0.4	1.5	−3.3	−0.2	−2.4
		Cl-SB$_{11}$				
A-B	−4.9	−3.5	5.6	−6.7	−0.9	−5.5
A-C	−3.9	−1.5	2.9	−6.1	−0.3	−5.0
A-D	−3.8	−1.5	3.9	−6.5	−0.5	−4.6
		I-SB$_{11}$				
A-B	−5.4	−3.5	6.6	−8.4	−1.1	−6.4
A-C	−4.3	−1.7	3.2	−6.7	−0.4	−5.6
A-D	−3.4	−0.8	3.4	−6.5	−0.5	−4.3

[a] $E^{\text{ind}} = E_2^{\text{ind}} + E_2^{\text{exch-ind}} + \delta\text{HF}$.

The interaction energies of the binding motifs found in the crystals are shown in Table 2. The strongest ΔE (−8.2 kcal mol^{-1}) was found for the A-B motif of **Ph-SB$_{11}$**, characterized by the B−S⋯π chalcogen bond. The DFT-D3 results were verified by the benchmark CCSD(T)/complete basis set (CBS) calculations, with a fair agreement. Notice that the B12-S axes of two **Ph-SB$_{11}$** molecules are not perpendicular (B12-S-Ph angle is 155°), in agreement with the prediction of nonlinearity of the chalcogen bond of the thiaboranes. The ΔE in the A-C and A-D stacking motifs of **Ph-SB$_{11}$**, which have no chalcogen bond, are weaker (−7.4 and −5.5 kcal mol^{-1}, respectively). The A-E and A-F motifs are considerably less stable because of the longer distances between Ph and the thiaborane cage.

Passing Cl or I, the chalcogen bonds are disfavored by about 3 kcal mol^{-1} compared to Ph. The B−S⋯π chalcogen bond is thus considerably more stable than the B−S⋯X one. The most stable motif features the chalcogen bond in all the crystals studied. The other motifs have head-to-tail and stacking interactions, and their ΔE are only slightly weaker.

The total ΔE is decomposed here using the DFT-SAPT technique in order to determine the nature of the respective binding (Table 2). The total ΔE values at the DFT-SAPT level are all slightly more negative than the DFT-D3 ones. In the case of **Ph-SB$_{11}$**, the A-C motif became more stable than the chalcogen-bonded A-B motif but based on the comparison with the CCSD(T) values this is probably an artifact of the method. The chalcogen bond in the motifs is dominated by the dispersion energy. The electrostatic stabilization is also important. Further, the induction energy is systematically larger for structures with a chalcogen bond, because of charge transfer in this motif.

To summarize, the most stable binding motif in the crystal of **Ph-SB$_{11}$** corresponds to a very strong B−S⋯π chalcogen bond exceeding −8 kcal mol^{-1}. It is considerably stronger than known C−X⋯π X-bonds. For comparison, the ΔE of the trifluoroiodomethane..benzene complex, possessing the X-bond, is −3.9 kcal mol^{-1}.[21] Dominant stabilization of the chalcogen bond investigated comes from dispersion and electrostatic energies. The phenyl group occurs frequently in proteins (in phenylalanine). The chalcogen bond can thus be used for designing protein–ligand interactions as well as for crystal engineering.

Experimental Section

Syntheses, NMR spectroscopies, X-ray diffraction analysis, and quantum mechanical calculations: The synthetic procedure of **Ph-SB$_{11}$** is based on the iodination of *closo*-1-SB$_{11}$H$_{11}$ followed by Negeshi coupling with Br-benzene. The shielding tensor of **Ph-SB$_{11}$** was computed and ^{1}H along with ^{11}B NMR spectra were recorded. The X-ray diffraction structure was established. QM calculations were performed using this structure. All the details are given in the Supporting Information.

Received: June 4, 2014
Published online: July 25, 2014

Keywords: boranes · chalcogen bonds · crystal structures · sulfur · X-ray diffraction

[1] P. Sanz, M. Yanez, O. Mo, *J. Phys. Chem. A* **2002**, *106*, 4661–4668.

[2] D. B. Werz, R. Gleiter, F. Rominger, *J. Am. Chem. Soc.* **2002**, *124*, 10638–10639.

[3] M. Iwaoka, S. Takemoto, S. Tomoda, *J. Am. Chem. Soc.* **2002**, *124*, 10613–10620.

[4] W. Wang, B. Ji, Y. Zhang, *J. Phys. Chem. A* **2009**, *113*, 8132–8135.

[5] T. Clark, M. Hennemann, J. S. Murray, P. Politzer, *J. Mol. Model.* **2007**, *13*, 291–296.

[6] M. Iwaoka, S. Takemoto, M. Okada, S. Tomoda, *Chem. Lett.* **2001**, 132–133.

[7] F. T. Burling, B. M. Goldstein, *J. Am. Chem. Soc.* **1992**, *114*, 2313–2320.

[8] Y. Nagao, T. Hirata, S. Goto, S. Sano, A. Kakehi, K. Iizuka, M. Shiro, *J. Am. Chem. Soc.* **1998**, *120*, 3104–3110.

[9] J. C. Taylor, G. D. Markham, *J. Biol. Chem.* **1999**, *274*, 32909–32914.

[10] K. Bender, I. Hennig, D. Schweitzer, *Mol. Cryst. Liq. Cryst.* **1984**, *108*, 359–371.

[11] a) M. Kolář, J. Hostaš, P. Hobza, *Phys. Chem. Chem. Phys.* **2014**, *16*, 9987–9996; b) R. Wilcken, M. O. Zimmermann, A. Lange, A. C. Joerger, F. M. Boeckler, *J. Med. Chem.* **2013**, *56*, 1363–1388.

[12] K. E. Riley, J. S. Murray, J. Fanfrlík, J. řezáč, R. J. Sola, M. C. Concha, F. M. Ramos, P. Politzer, *J. Mol. Model.* **2011**, *17*, 3309–3318.

[13] L. A. Hardegger, B. Kuhn, B. Spinnler, L. Anselm, R. Ecabert, M. Stihle, B. Gsell, R. Thoma, J. Diez, J. Benz, et al., *Angew. Chem.* **2011**, *123*, 329–334; *Angew. Chem. Int. Ed.* **2011**, *50*, 314–319.

[14] J. Fanfrlík, M. Kolář, M. Kamlar, D. Hurny, F. X. Ruiz, A. Cousido-Siah, A. Mitschler, J. Řezáč, E. Munusamy, M. Lepšík, et al., *ACS Chem. Biol.* **2013**, *8*, 2484–2492.

[15] a) N. S. Hosmane, *Boron Science*, CRC, Boca Raton, FL, **2011**; b) T. Baše, Z. Bastl, Z. Plzák, T. Grygar, J. Plešek, V. Malina, J. Šubrt, J. Boháček, E. Večerníková, O. Kříž, *Langmuir* **2005**, *21*, 7776–7785.

[16] P. Cígler, M. Kožíšek, P. Řezáčová, J. Brynda, Z. Otwinowski, J. Pokorná, J. Plešek, B. Grüner, L. Dolečková-Marešová, M. Máša, et al., *Proc. Natl. Acad. Sci. USA* **2005**, *102*, 15394–15399.

[17] J. Brynda, P. Mader, V. Šícha, M. Fábry, K. Poncová, M. Bakardiev, B. Grüner, P. Cígler, P. Řezáčová, *Angew. Chem.* **2013**, *125*, 14005 – 14008; *Angew. Chem. Int. Ed.* **2013**, *52*, 13760 – 13763.
[18] J. Fanfrlík, M. Lepšík, D. Horinek, Z. Havlas, P. Hobza, *ChemPhysChem* **2006**, *7*, 1100 – 1105.
[19] Z. F. Chen, R. B. King, *Chem. Rev.* **2005**, *105*, 3613 – 3642.
[20] J. Macháček, J. Plešek, J. Holub, D. Hnyk, V. Všetečka, I. Císařová, M. Kaupp, B. Štíbr, *Dalton Trans.* **2006**, *8*, 1024 – 1029.
[21] J. Řezáč, K. E. Riley, P. Hobza, *J. Chem. Theory Comput.* **2012**, *8*, 4285 – 4292.